Supplemental Figures:

Figure S1: Growth rate and bulk translation measurements are reproducible, show that *rp* mutants with lower growth rates have less translation, modest strictly growth-linked translation signatures, Related to Figures 1, 2, and 3. A) Reproducibility of growth rate measurements (as determined by OD600 measurements) was tested for a subset of *rp* mutants (full biological replicates) and found to be extremely highly reproducible by Pearson correlation. B) Our growth rate measurements for *rp* mutants in diploids in the SK1 strain background were highly correlated (Pearson) with measurements from another group (Steffen et al., 2012) in haploids of the S288C strain background. C) Our ^{35}S-methionine incorporation measurements were reproducible, based on Pearson correlation. Full biological replicates were tested for ^{35}S-methionine incorporation as a proxy for bulk translation rate, compared to WT controls. D) Both *rpl* and *rps* mutants show lower bulk translation associated with lower growth rate. *rpl* data is also shown in Figure 1B. Pearson correlation analysis was used. E) Ribosome profiling from a panel of wild-type, *rpl* and *rps* mutants was performed. Mutants were sorted according to growth rate and subjected to hierarchical clustering. Note that trends in gene expression are less apparent than in Figure 2A, which plots the same data, but divided by *rpl* or *rps* status. Note that columns (genes) are normalized to enable visual comparison among them. Enrichment based on H-B analysis of GO categories is shown below. F) Steady-state TE distributions do not change in RP-defective cells. The TE value distributions for two wild-type, two growth-defective *rpl*, and two

growth-defective *rps* mutants are shown. Note no significant difference in these constitutive nulls based on two-tailed Mann-Whitney analysis.

Figure S1

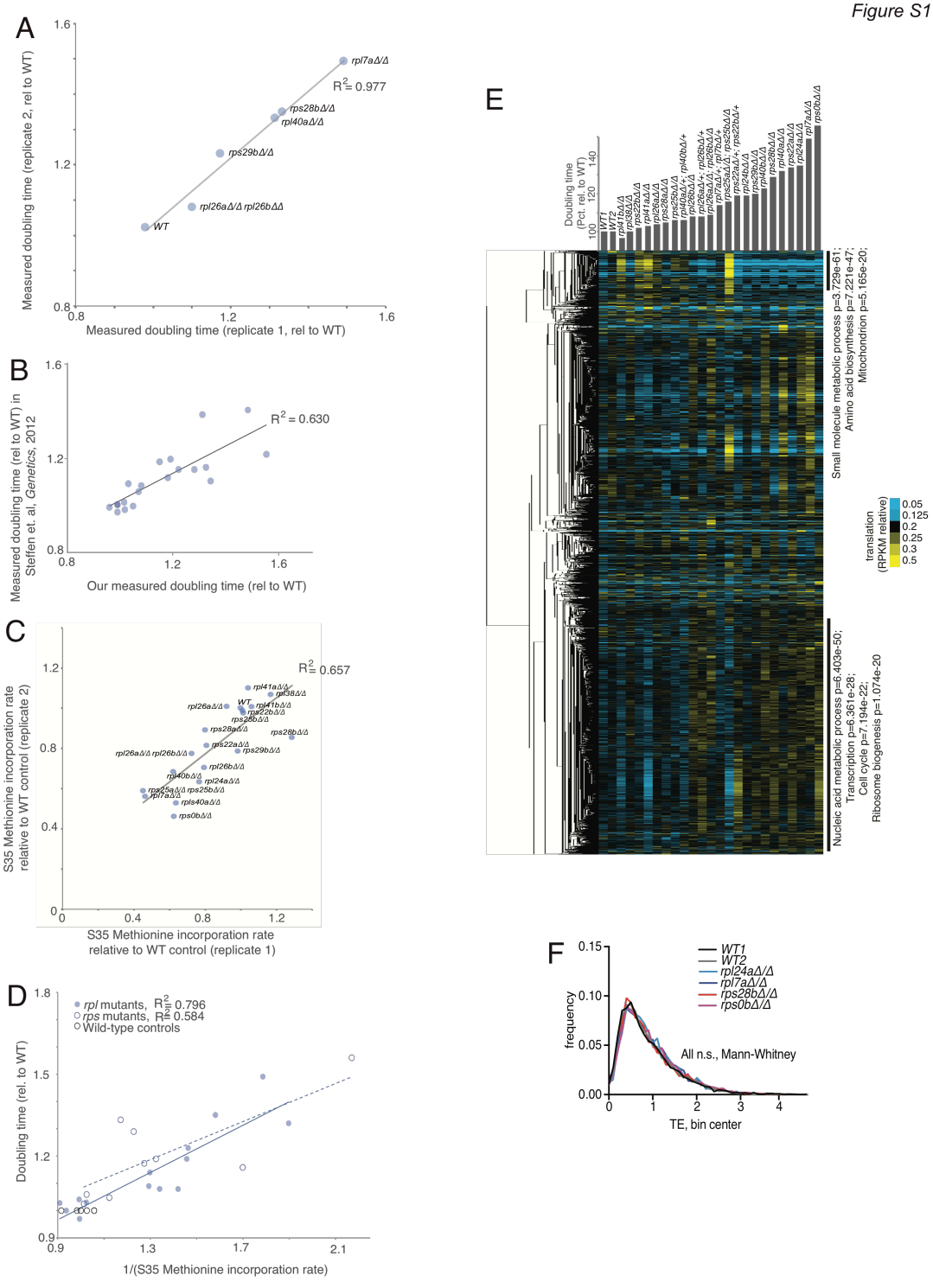
A
Measured doubling time (replicate 2, rel to WT)
Measured doubling time (replicate 1, rel to WT)
R2= 0.977
rpl7aΔ/Δ
rps28bΔ/Δ
rpl40aΔ/Δ
rps29bΔ/Δ
rpl26aΔ/Δ rpl26bΔΔ
WT
B
Measured doubling time (rel to WT) in Steffen et. al, Genetics, 2012
Our measured doubling time (rel to WT)
R2 = 0.630
C
S35 Methionine incorporation rate relative to WT control (replicate 2)
S35 Methionine incorporation rate relative to WT control (replicate 1)
R2= 0.657
D
rpl mutants, R2= 0.796
rps mutants, R2= 0.584
Wild-type controls
Doubling time (rel. to WT)
1/(S35 Methionine incorporation rate)
E
Doubling time (Pct. rel. to WT)
translation (RPKM relative)
Small molecule metabolic process p=3.729e-61;
Amino acid biosynthesis p=7.221e-47;
Mitochondrion p=5.165e-20;
Nucleic acid metabolic process p=6.403e-50;
Transcription p=6.361e-28;
Cell cycle p=7.194e-22;
Ribosome biogenesis p=1.074e-20
F
frequency
TE, bin center
WT1
WT2
rpl24aΔ/Δ
rpl7aΔ/Δ
rps28bΔ/Δ
rps0bΔ/Δ
All n.s., Mann-Whitney

Figure S2: Mass spectrometry of 80S/monosome fractions reveals similar RP composition for assembled ribosomes among *rp* mutants, Related to Figures 1-4, File S3. TMT mass spectrometry was performed on fractions corresponding to position of 80S/monosomes during polysome analysis by sucrose gradient. Rows (proteins/genes) were clustered hierarchically for each mutant relative to the same WT sample in each case, matched to the appropriate TMT mix. Circled boxes represent changes in levels of either the protein encoded by the deleted gene or its paralog in cases in which these RPs were quantified by mass spectrometry. Note the case of Rpl7, for which we measured each paralogous gene encoding this RP and note that in cells deleted for *RPL7A,* an increase in ribosome incorporation of Rpl7B could be seen.

Figure S2

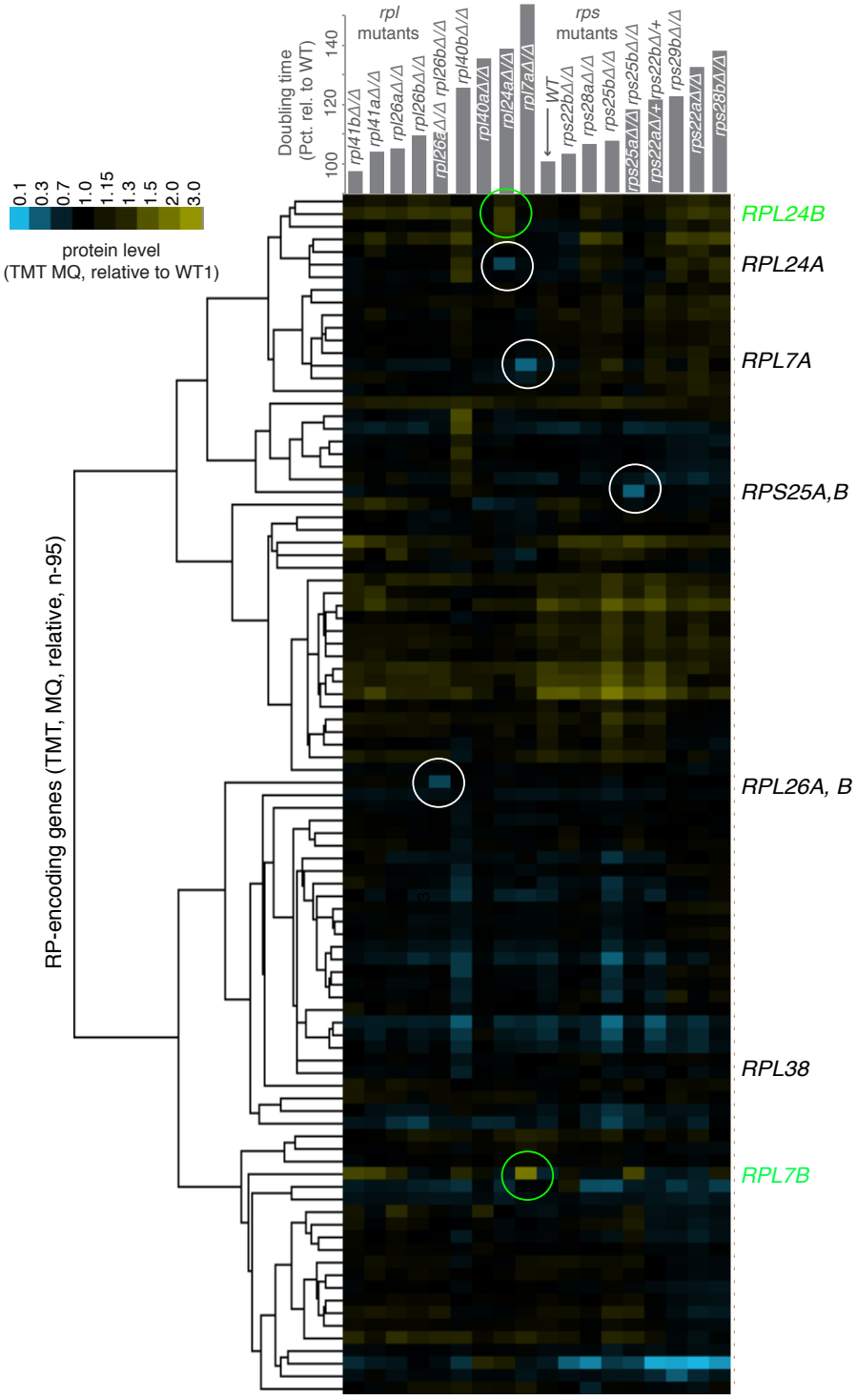
Doubling time
(Pct. rel. to WT)
100
120
140
rpl
mutants
rps
mutants
rpl41bΔ/Δ
rpl41aΔ/Δ
rpl26aΔ/Δ
rpl26bΔ/Δ
rpl26Δ/Δ rpl26bΔ/Δ
rpl40bΔ/Δ
rpl40aΔ/Δ
rpl24aΔ/Δ
rpl7aΔ/Δ
WT
rps22bΔ/Δ
rps28aΔ/Δ
rps25bΔ/Δ
rps25bΔ/Δ
rps25aΔ/Δ
rps22aΔ/+ rps22bΔ/+
rps29bΔ/Δ
rps22aΔ/Δ
rps28bΔ/Δ
0.1
0.3
0.7
1.0
1.15
1.3
1.5
2.0
3.0
protein level
(TMT MQ, relative to WT1)
RP-encoding genes (TMT, MQ, relative, n-95)
RPL24B
RPL24A
RPL7A
RPS25A,B
RPL26A, B
RPL38
RPL7B

Figure S3: Mass spectrometry of 60S polysome gradient fractions and rRNA analyses reveal specific enrichment for Rpl proteins in *rps* mutants, Related to Figure 5. A) TMT mass spectrometry was performed on fractions corresponding to position of 60S ribosomal subunits during polysome analysis by sucrose gradient. Columns (proteins/genes) were clustered hierarchically and each column was normalized to enable visual comparison among them. Note that *rps* mutants are enriched for a cluster of genes that are extremely highly enriched for large subunit RPs, based on H-B p-value analysis of GO enrichment. B-G) For all RNA species analyzed, total RNA sequencing results were aligned and quantified, order of strains is identical to Figure 2 and ratios are relative to WT. B) The ratio of total 25S versus 18S are shown. C) The ratio of reads from the 25.5S spacer region to 25S are shown. Note no enrichment in *rps* mutants, despite an overall high level of large subunit rRNA. D) The ratio of reads from the 7S spacer region to 5.8S are shown. E) The ratio of reads from the 20S spacer region to 18S are shown. Note that *rps29bΔ* and *rps0bΔ* cells show evidence of small subunit processing defects, consistent with published reports (Ferreira-Cerca et al., 2005; Ford et al., 1999; O'Donohue et al., 2010). F) The ratio of reads from the 5' ETS region to 18S, 5.8S, and 25S are shown. G) The ratio of reads from ITS2 to 25S are shown. H) Northern blotting for rRNA intermediates [as in (Babiano and de la Cruz, 2010)] is shown, reflecting similar trends as sequencing analyses in A-F. Note that 21S and 23S intermediates are described in (Martin-Marcos et al., 2007; Tabb-Massey, 2003).

Figure S3

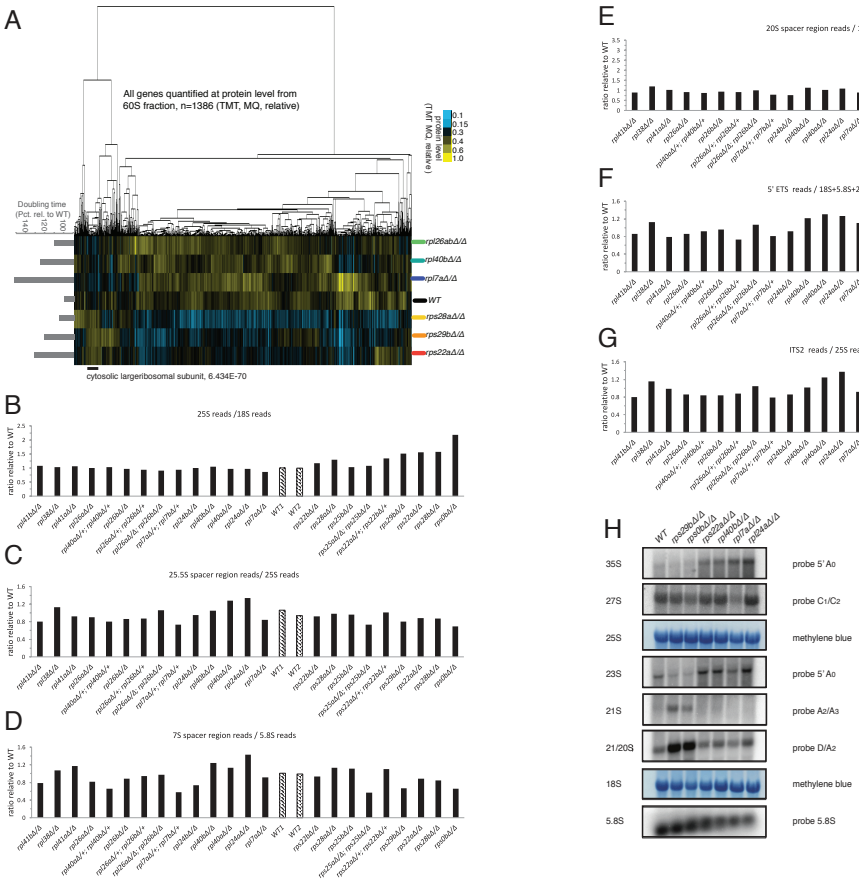
A
All genes quantified at protein level from 60S fraction, n=1386 (TMT, MQ, relative)
Doubling time (Pct. rel. to WT)
Protein level (TMT MQ, relative)
rpl26abΔ/Δ
rpl40bΔ/Δ
rpl7aΔ/Δ
WT
rps28aΔ/Δ
rps29bΔ/Δ
rps22aΔ/Δ
cytosolic largeribosomal subunit, 6.434E-70
B
25S reads /18S reads
C
25.5S spacer region reads/ 25S reads
D
7S spacer region reads / 5.8S reads
E
20S spacer region reads / 18S reads
F
5' ETS reads / 18S+5.8S+25S reads
G
ITS2 reads / 25S reads
ratio relative to WT
H
WT
rps28bΔ/Δ
rps29bΔ/Δ
rps22aΔ/Δ
rpl26abΔ/Δ
rpl7aΔ/Δ
rpl24aΔ/Δ
35S
27S
25S
23S
21S
21/20S
18S
5.8S
probe 5' A0
probe C1/C2
methylene blue
probe 5' A0
probe A2/A3
probe D/A2
methylene blue
probe 5.8S

Figure S4: Temperature-sensitivity and cell cycle defects in select *rp* mutants, Related to Figures 1-4. A) *rpl38Δ* cells show no growth defect at 30°C, but a profound growth defect at 37°C that is not shared by other *rpl* mutants. Cells were grown to exponential phase and plated in dilutions decreasing by 5-fold per spot from left to right. Identical cells were plated in parallel on two sets of plates and grown for either one or two days at either 30°C or 37°C. B) The results of flow cytometry on Sytox Green-treated wild-type and *rp* mutant cells show that growth defective *rpl* and *rps* mutants show G1 accumulation relative to WT controls. C) The results shown in B) were quantified according to DNA content.

Figure S4

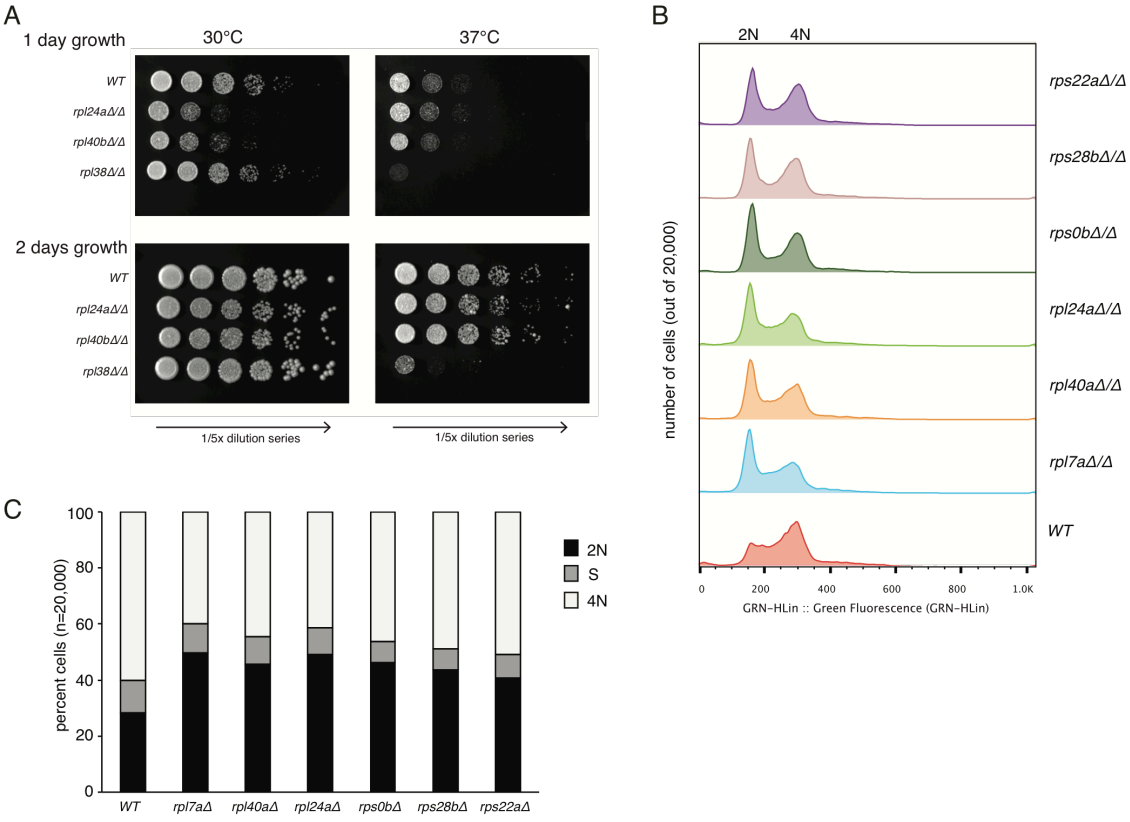
A
1 day growth
30°C
37°C
WT
rpl24aΔ/Δ
rpl40bΔ/Δ
rpl38Δ/Δ
2 days growth
WT
rpl24aΔ/Δ
rpl40bΔ/Δ
rpl38Δ/Δ
1/5x dilution series
1/5x dilution series
B
2N
4N
rps22aΔ/Δ
rps28bΔ/Δ
rps0bΔ/Δ
rpl24aΔ/Δ
rpl40aΔ/Δ
rpl7aΔ/Δ
WT
number of cells (out of 20,000)
0
200
400
600
800
1.0K
GRN-HLin :: Green Fluorescence (GRN-HLin)
C
percent cells (n=20,000)
100
80
60
40
20
0
2N
S
4N
WT
rpl7aΔ
rpl40aΔ
rpl24aΔ
rps0bΔ
rps28bΔ
rps22aΔ

Figure S5: mRNA-seq, ribosome profiling, and mass spectrometry measurements were reproducible and showed expected correlations, Related to Figures 1-4; Files S1, S2, and S4; STAR Methods. A-C) The results of gene expression measurements for full biological replicates for wild-type cells grown in parallel with *rp* mutants analyzed in Figures 1, 2, 3, and 4 are shown and compared using Pearson correlation-based analysis. A) ribosome profiling measurements of translation are highly reproducible in our experiments. B) mRNA-seq measurements are highly reproducible in our experiments. C) TMT-based mass spectrometry measurements of protein levels are highly reproducible in our experiments. D) Correlations among mRNA, ribosome profiling and mass spectrometry measurements. Pearson correlation coefficients are shown between each type of gene expression measurement for each strain for which we measured mRNA, translation (by ribosome footprints, abbreviated "FP"). To allow comparison to mass spectrometry data, values were first multiplied by average iBAQ value for each sample mixture.

Figure S5

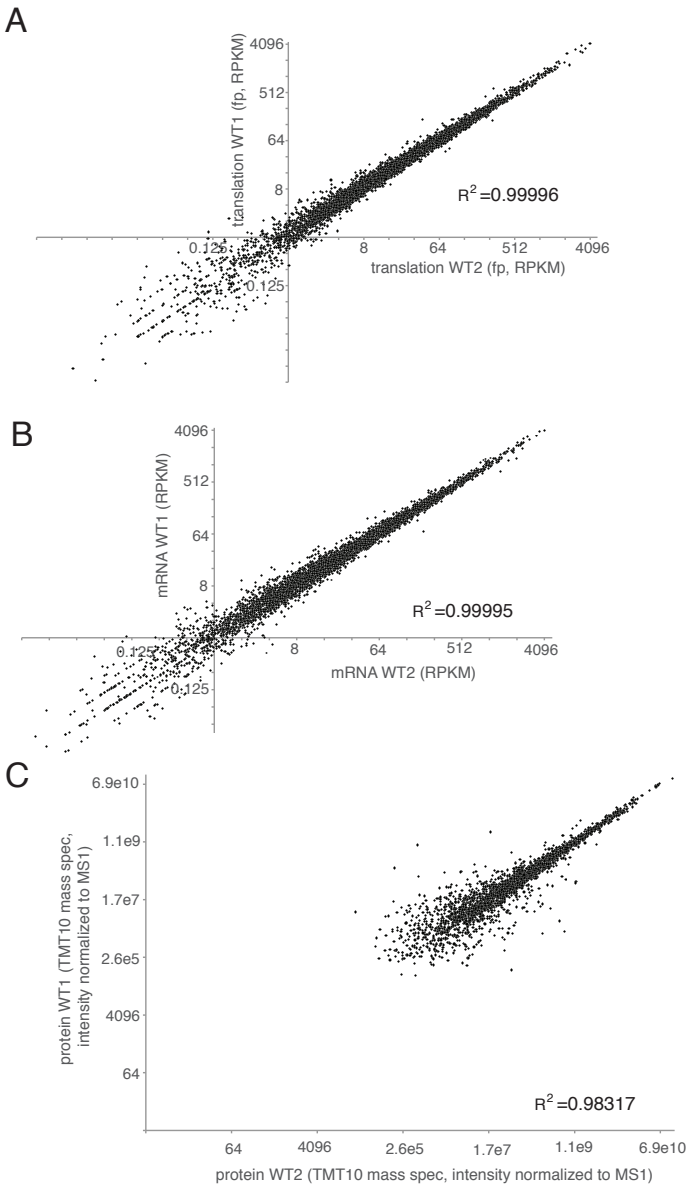

D

	rpl41bΔ	*rpl38Δ*	*rpl41aΔ*	*rpl26aΔ*	*rpl26bΔ*	*rpl26aΔ rpl26bΔ*	*rpl40bΔ*	*rpl40aΔ*	*rpl24aΔ*	*rpl7aΔ*	*WT*	*rps22bΔ*	*rps28aΔ*	*rps25aΔ rps25bΔ*	*rps25aΔ rps26bΔ*	*rps29bΔ*	*rps22aΔ*	*rps28bΔ*	*rps0bΔ*
FP:RNA	0.843	0.871	0.861	0.875	0.864	0.884	0.853	0.842	0.861	0.849	0.865	0.833	0.865	0.859	0.833	0.854	0.835	0.838	0.817
FP:Prot	0.573	0.530	0.586	0.505	0.485	0.494	0.504	0.487	0.502	0.507	0.526	0.563	0.520	0.530	0.572	0.516	0.477	0.503	0.437
RNA:Prot	0.329	0.337	0.356	0.322	0.326	0.338	0.321	0.305	0.346	0.324	0.328	0.298	0.324	0.328	0.303	0.293	0.277	0.287	0.223

Key 0.20 0.30 0.40 0.50 0.60 0.70 0.80 0.90 Correlation coefficient (Pearson)